Single-photon scattering and bound states in a one-dimensional waveguide with a topological giant atom

Wei Zhao,[1] Tian Tian,[2] and Zhihai Wang[1,*]

[1]*Center for Quantum Sciences and School of Physics, Northeast Normal University, Changchun 130024, China*

[2]*School of Materials Science and Engineering, Changchun University, Changchun 130022, China*

(Received 8 January 2024; accepted 3 June 2024; published 17 June 2024)

We investigate the single-photon scattering and bound states in a coupled resonator waveguide (CRW) which couples to a topological giant atom (TGA) via two distant sites. Here, the TGA is constructed by a one-dimensional Su-Schrieffer-Heeger chain with a finite length. By modulating the topological phase of the TGA, the incident photon in the CRW can be completely reflected or transmitted, and is therefore beneficial to designing a coherent photonic device. Meanwhile, we also achieve two pairs of bound states locating respectively above and below the continuum. Whether the gap is open or closed depends on the boundary condition of the TGA. Therefore, the combination of topology and interference provides us with an exciting opportunity to manipulate the photonic state in the context of waveguide quantum electrodynamics.

DOI: 10.1103/PhysRevA.109.063708

I. INTRODUCTION

The light-matter interaction plays a crucial role in the fundamental sciences [1,2], underpinning the rapid development of quantum technology. Recently, the light-matter interaction in waveguide structures has attracted much attention and led to many theoretical [3] and experimental studies in the waveguide quantum electrodynamics (QED) [4] community, such as dressed or bound states [5–11], phase transitions [12,13], single-photon devices [14–16], and exotic topological and chiral phenomena [17–22]. At the same time, the dynamical control of single-photon transmission is a hot topic in constructing quantum networks [23], since photons provide a reliable output of quantum information and the single photon is considered to be one of the most suitable carriers of quantum information. In quantum devices and quantum networks [24–26], one-dimensional (1D) waveguides [27,28] are essential light-matter interfaces, and controllable single-photon transport with linear and nonlinear dispersion relationships has been extensively studied [29–31].

In the traditional treatment, the light-matter interaction is often modeled by the dipole approximation, where the atoms are treated as pointlike dipoles [32]. However, recently, the study of the interaction in atom-waveguide systems has been extended to the interaction between the photon and giant atom(s), where the nonlocal light-matter interaction occurs with multiple points. In the giant atom community [33–41], since the interactions between the waveguide photons and the giant atoms include multipath quantum interferences, many new phenomena that do not exist in traditional small atom systems have been predicted, such as a tunable bound state [42–45], decoherence-free interaction [46], electromagnetically induced transparency [47,48], Autler-Townes splitting phenomena [49], chiral physics [50–54], and many others [55–57]. The physical basis behind these phenomena is the interference and delay effects in the propagation of the photon/phonon between different coupling points.

On the other hand, Haldane and Raghu [58,59] proposed to manipulate the photon transport via a topological structure in 2008, which paved the way for the development of topological photonics [60–67]. In the simplest one-dimensional case, a topological waveguide can be constructed [68,69] through a Su-Schrieffer-Heeger (SSH) [70] chain, which is characterized by a nonzero winding number or zero-mode edge state(s) in a topologically nontrivial phase with a periodic boundary condition (PBC) or open boundary condition (OBC), respectively [71–74]. Especially, an edge state in a one-dimensional SSH chain has been experimentally observed, and the localization length has been extracted in terms of survival probability in Ref. [75].

Therefore, combining the unique effect of the nonlocal light-matter interaction in giant atom quantum optics and the robust natural effect of the topological photonics, we here investigate the manipulation of a single-photon state in the context of waveguide QED. To this end, we couple a one-dimensional SSH chain with a finite length to an infinite coupled resonator waveguide (CRW), to study the photonic scattering and dressing state in a single excitation level. Since a short topological SSH chain supports a few discrete energy levels and couples to the CRW via two distant sites, in what follows, we refer to it as a topological giant atom (TGA). Thus, the topological nature of the TGA is utilized to adjust the photon state in the CRW. Our findings imply that single-photon scattering can be modulated by the topological phase of the TGA and the bound state is controlled by its boundary conditions.

II. MODEL AND HAMILTONIAN

As schematically shown in Fig. 1, the system we consider is composed of two arrays of CRW. The upper one is an

*Contact author: wangzh761@nenu.edu.cn

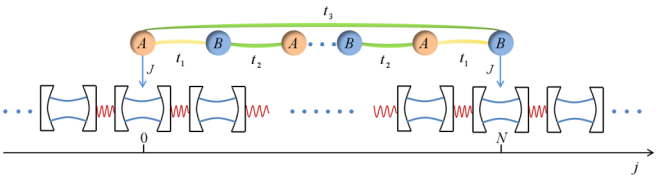

FIG. 1. Schematic diagram of coupling of a TGA to an infinite CRW via two coupling points. The upper part is a TGA formed by a finite SSH chain with t_1 and t_2 being the intra- and intercell hopping amplitudes, respectively, and t_3 is the cyclic hopping amplitude. The lower part is an infinite CRW. The TGA coupled to the CRW via two separate sites of $j = 0$ and $j = N$, and the coupling strengths for the two sites are both J.

$N + 1$ site [i.e., $(N + 1)/2$ pairs for odd N] SSH chain and the lower one is an infinite CRW with a uniform photonic hopping strength. The upper SSH chain supports finite discrete energy levels and serves as the TGA, whose topological nature is discussed below. The TGA couples to the CRW nonlocally via two separate sites of $j = 0$ and $j = N$. The Hamiltonian H of the system can be divided into three parts, i.e., $H = H_c + H_S + H_I$.

The first part, H_c, represents the free Hamiltonian of the CRW, and is expressed as

$$H_c = \omega_c \sum_j a_j^\dagger a_j - \xi \sum_{j=-\infty}^{+\infty} (a_{j+1}^\dagger a_j + a_j^\dagger a_{j+1}), \tag{1}$$

where ω_c is the bare frequency of the resonators and $a_j^\dagger$ (a_j) is the bosonic creation (annihilation) operator on site j, which satisfies the commutation relation $[a_j, a_j^\dagger] = 1$. ξ is the hopping strength between the nearest resonators.

The second part, H_S, of the Hamiltonian H represents the free Hamiltonian of the TGA [consisting of L unit cells, $L = (N + 1)/2$ for odd N], which can be written as

$$\begin{aligned} H_S = &\sum_{l=1}^{L} \omega_e (C_{A,l}^\dagger C_{A,l} + C_{B,l}^\dagger C_{B,l}) + t_1 \sum_{l=1}^{L} (C_{A,l}^\dagger C_{B,l} + \text{H.c.}) \\ &+ t_2 \sum_{l=1}^{L-1} (C_{A,l+1}^\dagger C_{B,l} + \text{H.c.}) + t_3 (C_{A,1}^\dagger C_{B,L} + \text{H.c.}). \end{aligned} \tag{2}$$

In the TGA, each unit cell hosts two resonators A and B with an identical frequency ω_e, and $C_{A,l}$ ($C_{B,l}$) is the bosonic annihilation operator at the A (B) sublattices of the lth unit cell (see Fig. 1). The intra- and intercell hopping amplitudes are t_1 and t_2, respectively. Here, we use the value of t_3 to distinguish between the boundary condition of the TGA. For the PBC, we set $t_3 = t_2$. In the case of PBC, the topological phase transition is characterized by the winding number w. In the topologically trivial phase ($|t_1| > |t_2|$), the winding phase is $w = 1$. Otherwise, in the the topologically nontrivial phase ($|t_1| < |t_2|$), the winding phase is $w = 0$. For the OBC, we set $t_3 = 0$, and the TGA supports the boundary state in the topologically nontrivial phase, but not in the trivial phase.

The third part H_I of the Hamiltonian describes the coupling between the TGA and the CRW via the zeroth and Nth resonators with the same coupling strength J. Under the rotating-wave approximation, the Hamiltonian H_I can be written as

$$H_I = J(a_0^\dagger C_{A,1} + a_N^\dagger C_{B,L} + \text{H.c.}). \tag{3}$$

III. SINGLE-PHOTON SCATTERING

In this section, we will discuss the behavior of single-photon scattering by an open TGA ($t_3 = 0$). We consider that a single photon with wave vector k is incident from the left side of the waveguide. Since the excitation number in the system is conserved, the eigenstate in the single-excitation subspace can be written as

$$|E_k\rangle = \sum_j U_j a_j^\dagger |G\rangle + \sum_l X_l C_{A,l}^\dagger |G\rangle + \sum_l Y_l C_{B,l}^\dagger |G\rangle, \tag{4}$$

where $|G\rangle$ represents that all of the resonators in the CRW and TGA are in their vacuum states. U_j is the probability amplitude for finding a photonic excitation in site j of the CRW, and X_l (Y_l) describe the excitation amplitudes in site A_l (B_l) of the TGA. In the regimes of $j < 0$, $0 \leqslant j \leqslant N$, and $j > N$, the amplitude U_j can be written in the form

$$U_j = \begin{cases} e^{ikj} + re^{-ikj}, & j < 0, \\ Ae^{ikj} + Be^{-ikj}, & 0 \leqslant j \leqslant N, \\ te^{ikj}, & j > N, \end{cases} \tag{5}$$

where r and t are respectively the single-photon reflection and transmission amplitudes. Furthermore, the second line in the above equation implies that the incident photon can be transmitted (reflected) by the left (right) leg of the TGA with amplitude A (B). The transmitted photon then propagates back and forth in the spatial regime covered by the TGA with $0 \leqslant j \leqslant N$.

Solving the Schrödinger equation $H|E_k\rangle = E|E_k\rangle$ in the region of $j \neq 0, N$, it yields a dispersion relationship of $E_k = \omega_c - 2\xi \cos k$. Furthermore, the continuity conditions at $j = 0$ and $j = N$ give $1 + r = A + B$ and $Ae^{ikN} + Be^{-ikN} = te^{ikN}$, respectively.

We begin with the simplest case with $N = 1$, in which the TGA is composed of one A site and one B site as shown in Fig. 2(a). An analytical expression for the reflection amplitude r can be obtained as

$$\begin{aligned} r = &\frac{i\xi(\Delta_2 + t_1)\sin k}{[\Delta_1 + \xi(e^{ik} - 1)](\Delta_2 + t_1) - J^2} \\ &+ \frac{i\xi(\Delta_2 - t_1)\sin k}{[\Delta_1 + \xi(e^{ik} + 1)](\Delta_2 - t_1) - J^2} - 1, \end{aligned} \tag{6}$$

where $\Delta_1 = E_k - \omega_c$ and $\Delta_2 = E_k - \omega_e$ represent the detuning between the propagating photon in the waveguide and the bare resonators in the CRW and the TGA, respectively. Since spontaneous radiation for all of the resonators is ignored, it satisfies that $R + T = 1$, where $R = |r|^2$ is the reflection rate and $T = |t|^2$ is the transmission rate.

In Fig. 2(c), we demonstrate the reflection rate R as a function of photon-atom detuning Δ_2 in the resonance condition, that is, $\omega_c = \omega_e$. The result for the scheme of a single cell [$N = 1$ shown in Fig. 2(a)] is illustrated by the blue solid curve. The two complete reflection peaks ($R = 1$) characterize

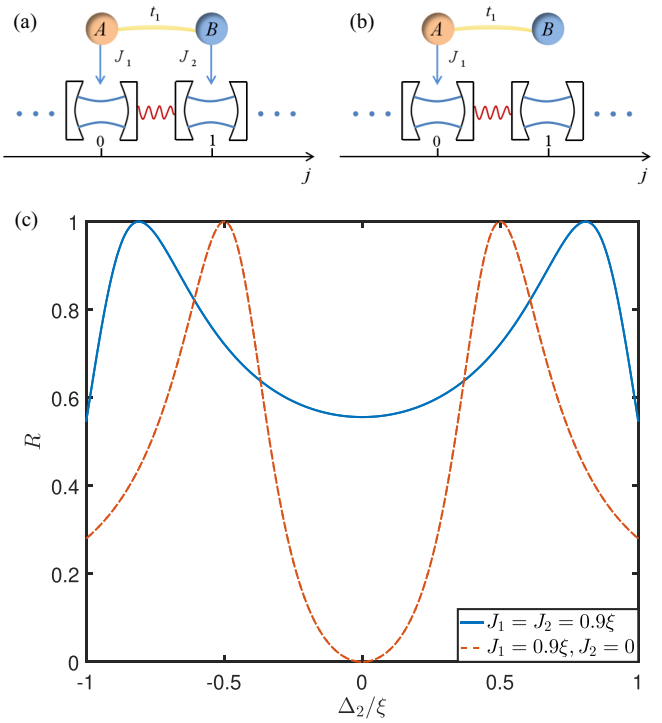

FIG. 2. (a) Schematic diagram of the model when $N = 1$. (b) Schematic diagram of TGA where only one of the two sites is coupled to CRW via one resonator. (c) The reflection rate R as a function of detuning Δ_2 for $N = 1$. The parameters are set as $t_1 = 0.5\xi$, $\omega_e = \omega_c = 20\xi$.

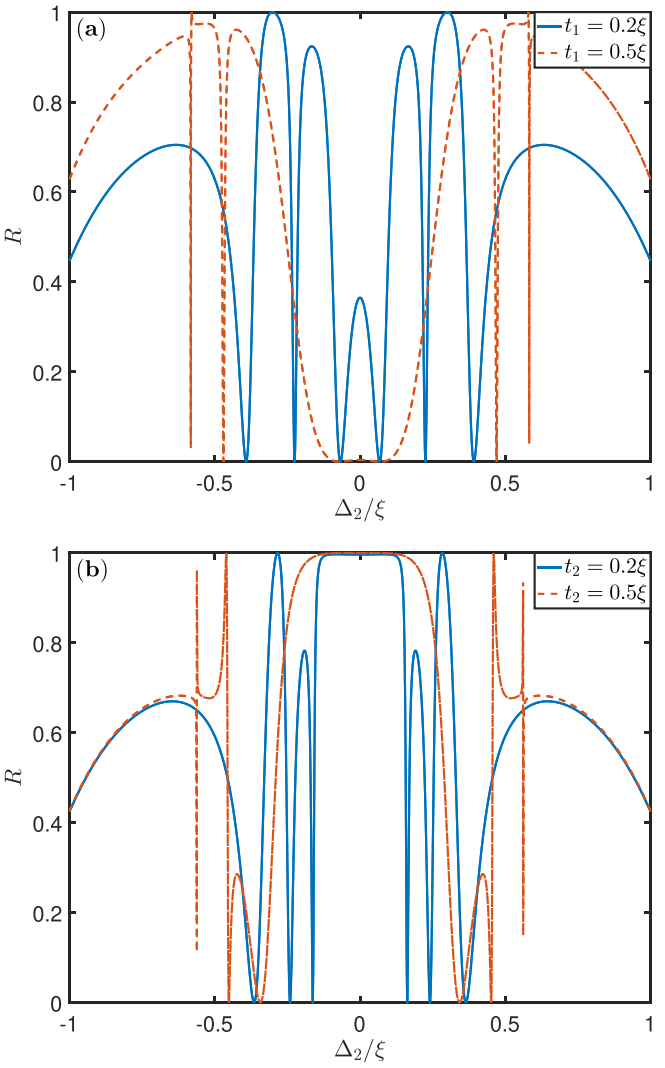

FIG. 3. The reflection rate R as a function of detuning Δ_2 for $N = 5$, and (a) $t_2 = 0.1\xi$, (b) $t_1 = 0.1\xi$. The parameters are set as $J = 0.9\xi$, $\omega_e = \omega_c = 20\xi$.

the intercoupling inside the TGA. Moreover, when only one of the two sites in the TGA couples to one resonator in the lower CRW [shown in Fig. 2(b)], the single-photon reflection is characterized by the Rabi splitting behavior. As shown in the figure, the peaks of the orange dashed line locate exactly at the frequency $\Delta_2 = \pm t_1$. The deviation from the Rabi splitting for the two sites being coupled originates from the photonic interference effect when it propagates back and forth, and this interference is peculiar for the giant atom setup.

Next, let us move to the case of $N > 1$, in which the topological properties of the TGA take effect. In Fig. 3, we demonstrate the reflection rate R for $N = 5$ as a function of the detuning Δ_2. As shown in the figures, the reflection rate shows a complicated behavior in the two-band regime of $-|t_1 + t_2| < \Delta_2 < -|t_1 - t_2|$ and $|t_1 - t_2| < \Delta_2 < |t_1 + t_2|$. In the gapped regime with $-|t_1 - t_2| < \Delta_2 < |t_1 - t_2|$, the reflection rate behaves differently when the TGA undergoes a topological phase transition. For example, in the topologically trivial phase ($t_1 > t_2$), we illustrate the results for $t_2 = 0.1\xi$ in the cases of $t_1 = 0.2\xi$ and $t_1 = 0.5\xi$, respectively, in Fig. 3(a). For small t_1 with $t_1 = 0.2\xi$, there exists a small peak at zero detuning $\Delta_2 = 0$. As t_1 increases, the peak is smoothed and it forms a relatively wideband for $R = 0$ near the regime of $\Delta_2 = 0$. It implies that the incident photon will be completely transmitted. This is due to the constructive interference caused by the photonic backward and forward propagation in the spatial regime covered by the TGA. It implies that the TGA in the topologically trivial phase can be used to realize quantum cloaking [76,77], that is, the presence of TGA has no effect on the propagation of the photon in the CRW. In other words, the photon in the CRW cannot "see" the TGA, i.e., the TGA is invisible. On the other hand, when the TGA works in the topologically nontrivial phase, the destructive interference between photons results in complete reflection and the reflection window ($R = 1$) is demonstrated in Fig. 3(b) near the resonant regime of $\Delta_2 = 0$.

The results in Fig. 3 indicate that we can use the TGA to construct the coherent single-photon device. When a value of order of 100 MHz of $t_{1(2)}$ is achieved experimentally [78], we can realize quantum cloaking or complete reflection with a bandwidth of about 100–200 MHz, which is in the same order of t_1 and t_2.

We continue our discussion by considering single-photon scattering when the bare resonator is not in resonance with the TGA. In Fig. 4, we demonstrate reflectance R as a function of photon-atom detuning Δ_2 under a nonresonant condition, i.e., $\omega_e \neq \omega_c$. The result of the single-cell scheme ($N = 1$) is illustrated by the solid blue line. The dotted orange and yellow lines represent the result in the topologically trivial

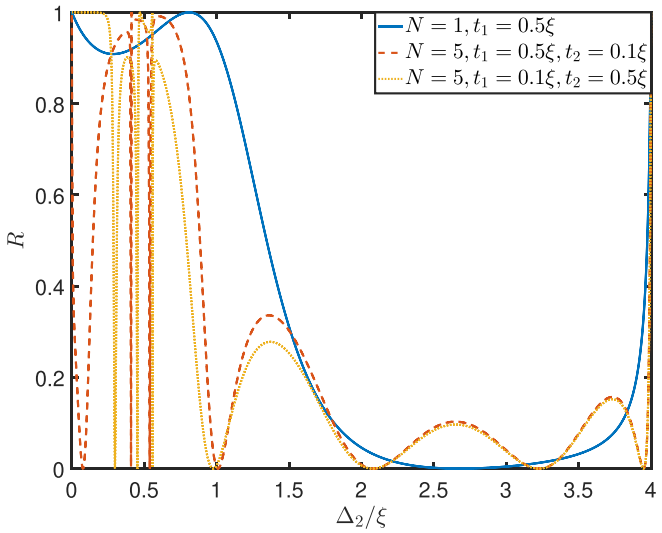

FIG. 4. The reflection rate R as a function of detuning Δ_2 when the bare resonator is off resonant with the TGA. The parameters are set as $J = 0.9\xi$, $\omega_e = 18\xi$, and $\omega_c = 20\xi$.

and nontrivial phase, respectively, for $N = 5$. We find that the asymmetric reflection curve is completely different from the resonance condition, and around the reflection point, the reflection yields a Fano shape [79,80]. With an increase of the size of the TGA, the reflection rate shows a complicated dependence on the detuning Δ_2. This means that off resonance we can induce Fano physics in such a hybrid system. We also observe that there will be one or more complete reflection frequencies (excluding the edge of the photonic propagation band), depending on the values of N. It implies that we can design on-demand single-photon transistors by adjusting the size of TGA in our waveguide QED setup.

IV. SINGLE-PHOTON BOUND STATE

In the previous section, we have studied the single-photon scattering states which locate inside the propagating band $E_k \in [\omega_c - 2\xi, \omega_c + 2\xi]$. Due to the coupling between the TGA and the CRW, the translational symmetry of the system is broken, leading to the photonic bound states which lie outside the propagating band. Here, we resort to numerical diagonalization of the Hamiltonian to find these bound states when the TGA works in the topologically nontrivial phase ($t_1 < t_2$).

In Figs. 5(a) and 5(b), we plot the energy spectrum by considering that the TGA works in the PBC ($t_3 = t_2$) and OBC ($t_3 = 0$), respectively. As expected, we observe a continual band which supports the propagating modes in both cases and a difference arises from the bound states outside the continuum. In the PBC, there exist two pairs of nondegenerate bound states, which locate symmetrically above and below the continuum and are denoted by E_1, E_2, E_3, and E_4, respectively, as shown in Fig. 5(a). Within the available experimental parameter $\xi = 100$ MHz, the gap between the gap state $\Delta_E = E_1 - E_2 = E_3 - E_4$ is in the order of 10 MHz in the condition of $J = 3\xi$. As a comparison, when the TGA works in the OBC, pairs of bound states become degenerate

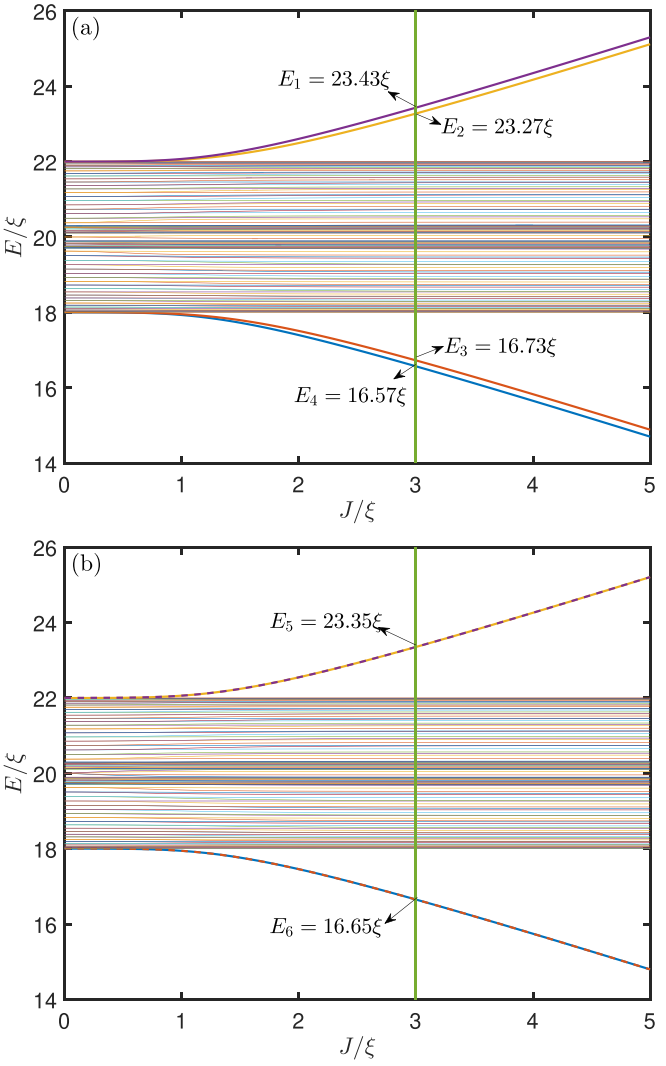

FIG. 5. The energy spectrum for $N = 29$ in (a) $t_3 = t_2$, and (b) $t_3 = 0$. The parameters are set as $t_1 = 0.1\xi$, $t_2 = 0.2\xi$, $\omega_e = \omega_c = 20\xi$.

as shown in Fig. 5(b). Moreover, it satisfies $E_5 = (E_1 + E_2)/2$ and $E_6 = (E_3 + E_4)/2$.

The above transition from degenerate bound states to nondegenerate ones provides an effective approach to detect the boundary condition of the TGA. To this end, we introduce an auxiliary probing atom whose resonant frequency satisfies $\omega_p = E_6$ and observe its excitation evolution. Then, the probing Hamiltonian is expressed as

$$H_p = H + (\omega_p - i\gamma)|e\rangle_p\langle e| + f(\tau_+ a_j + \text{H.c.}), \qquad (7)$$

which demonstrates that the probing atom is coupled to the jth cavity with the coupling strength f, and γ and $\tau_+ = |e\rangle_p\langle g|$ are the spontaneous emission and raising operator of the probing atom.

Preparing initially the probing atom in the excited state and the TGA-CRW coupled system in the ground state, we plot the excitation dynamics of the probing atom in Fig. 6 by taking $J = 3\xi$. Here, the probing atom is located in the resonator of $j = 0$, that is, the left leg of the TGA. Since the probing atom is large detuned from both bound states in the condition

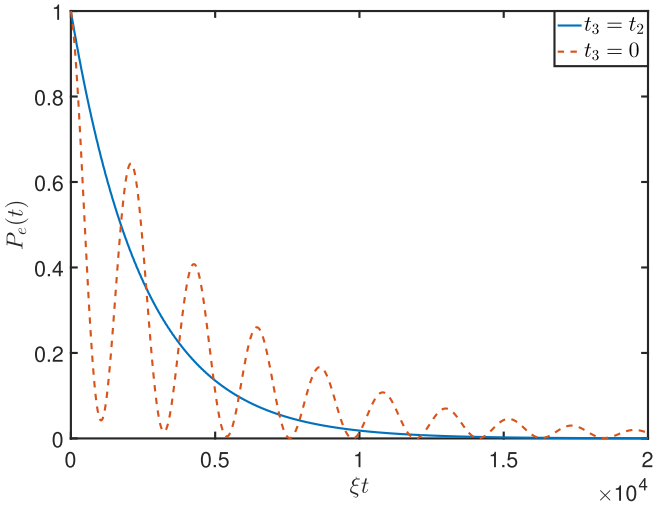

FIG. 6. The evolution of the population in the excited state for the probing atom for $t_2 = t_3$ (blue solid line), and $t_3 = 0$ (orange dashed line). The parameters are set as $N = 29$, $\omega_e = \omega_c = 20\xi$, $\omega_p = E_6 = 16.65\xi$, $t_1 = 0.1\xi$, $t_2 = 0.2\xi$, $J = 3\xi$, $f = 2 \times 10^{-3}\xi$, $\gamma = 2 \times 10^{-4}\xi$.

of $f \ll |\omega - E_{3(4)}|$, the probing atom is effectively decoupled from the TGA-CRW system in the PBC. As a result, the dynamics of $P_e(t) = \langle |e\rangle_p\langle e| \rangle$ shows an exponential decay, which is determined by the spontaneous dissipation rate γ as shown by the solid line in Fig. 6. In the OBC, a pair of nondegenerate bound states emerge into the degenerate ones, which resonate with the probing atom, so that the dynamics exhibits a Rabi oscillation character as shown by the dashed line. In this sense, the boundary condition of the TGA can be detected in a coherent manner.

V. REMARKS AND CONCLUSIONS

In this paper, we have constructed a TGA via a finite SSH chain which couples to the CRW. In the single excitation subspace, we discuss the scattering and bound states, respectively. We find that the photonic scattering behavior can be modulated by the topological nature of the TGA. Together with the interference effect during the propagation of the photon in the waveguide, we can design a wideband cloaking or reflection photonic device when the TGA works in the topologically trivial or nontrivial phases, respectively. As for the bound states which locate outside the continuum, the energy gap can be closed or opened, depending on the boundary condition of the TGA.

In the current experimental availability, the proposed model can be realized in superconducting circuits. In 2014, the first experiment which coupled the superconducting transmon quantum qubit and the surface acoustic wave (SAW) waveguide was realized. Here, the qubit is 20 times larger than the wavelength of the SAW in size and it therefore reached the giant atom regime [81]. This ratio between the size of the giant atom and the wavelength was then developed to 100 and the light-matter interaction was achieved by tens of MHz [37]. Additionally, a giant atom was also achieved by coupling artificial atoms created with Josephson junctions to superconducting circuits through capacitance or inductance. In Ref. [40], the giant atom was experimentally coupled to a waveguide at multiple, yet well-separated, locations. The distance between two coupling points could reach 20.54 mm [48]. Recently, the topology of two nested giant spin ensembles (GSEs) has been experimentally demonstrated, where the distance between the two inner (outer) coupling points is designed to be 8.3 (16.6) cm [82]. It provides a new platform for "giant atom" physics. Moreover, the CRW constructed with nine superconducting qubits is also realized in the experiment, where the nearest-neighbor coupling strength is $\xi/2\pi = 50$ MHz [83]. In a recent experiment, Painter's group expanded the CRW consisting of a 42 unit-cell array of capacitively coupled lumped-element microwave resonators [84], and a SSH topological structure was also constructed with a hopping strength $J(1 \pm \delta)$ where $J/2\pi = 368$ MHz, $\delta = 0.282$. Furthermore, the qubit-resonator coupling strength in such a structure was achieved by $g/2\pi = 124.6$ MHz [78]

The establishment of TGA in our work provides an unconventional approach to regulate the transmission and distribution of the single photon in the CRW. Here, the interference effect for the propagation of the photon in the regime of the giant atom will be applicable in quantum control and quantum information processing. We hope that our work of controlling photons through giant atom systems combined with topologies will stimulate further research into the hybrid system and broaden the range of application of artificial giant atoms.

ACKNOWLEDGMENTS

This work is supported by the funding from Jilin Province (Grants No. 20230101357JC and No. 20220502002GH) and the National Science Foundation of China (Grants No. 12105026 and No. 12375010).

[1] P. Forn-Díaz, L. Lamata, E. Rico, J. Kono, and E. Solano, Rev. Mod. Phys. **91**, 025005 (2019).
[2] R. Gutzler, M. Garg, C. R. Ast, K. Kuhnke, and K. Kern, Nat. Rev. Phys. **3**, 441 (2021).
[3] Y.-X. Zhang, C. R. i Carceller, M. Kjaergaard, and A. S. Sørensen, Phys. Rev. Lett. **127**, 233601 (2021).
[4] X. Gu, A. F. Kockum, A. Miranowicz, Y.-X. Liu, and F. Nori, Phys. Rep. **718-719**, 1 (2017).
[5] H. Zheng, D. J. Gauthier, and H. U. Baranger, Phys. Rev. A **82**, 063816 (2010).
[6] G. Calajó, F. Ciccarello, D. Chang, and P. Rabl, Phys. Rev. A **93**, 033833 (2016).
[7] T. Shi, Y.-H. Wu, A. González-Tudela, and J. I. Cirac, Phys. Rev. X **6**, 021027 (2016).
[8] E. Sánchez-Burillo, D. Zueco, L. Martín-Moreno, and J. J. Garcia-Ripoll, Phys. Rev. A **96**, 023831 (2017).

[9] P. T. Fong and C. K. Law, Phys. Rev. A **96**, 023842 (2017).
[10] G. Calajó, Y.-L. L. Fang, H. U. Baranger, and F. Ciccarello, Phys. Rev. Lett. **122**, 073601 (2019).
[11] W. Zhao and Z. Wang, Phys. Rev. A **101**, 053855 (2020).
[12] M. Fitzpatrick, N. M. Sundaresan, A. C. Y. Li, J. Koch, and A. A. Houck, Phys. Rev. X **7**, 011016 (2017).
[13] L. Qiao, Y.-J. Song, and C.-P. Sun, Phys. Rev. A **100**, 013825 (2019).
[14] J. T. Shen and S. Fan, Phys. Rev. Lett. **95**, 213001 (2005).
[15] D. E. Chang, A. S. Sørensen, E. A. Demler, and M. D. Lukin, Nat. Phys. **3**, 807 (2007).
[16] L. Zhou, Z. R. Gong, Y. X. Liu, C. P. Sun, and F. Nori, Phys. Rev. Lett. **101**, 100501 (2008).
[17] M. Ringel, M. Pletyukhov, and V. Gritsev, New J. Phys. **16**, 113030 (2014).
[18] V. Yannopapas, Int. J. Mod. Phys. B **28**, 1441006 (2014).
[19] I. M. Mirza and J. C. Schotland, Phys. Rev. A **94**, 012302 (2016).
[20] C. Gonzalez-Ballestero, E. Moreno, F. J. Garcia-Vidal, and A. Gonzalez-Tudela, Phys. Rev. A **94**, 063817 (2016).
[21] M. Bello, G. Platero, J. I. Cirac, and A. G. Tudela, Sci. Adv. **5**, eaaw0297 (2019).
[22] S. Mahmoodian, G. Calajó, D. E. Chang, K. Hammerer, and A. S. Sørensen, Phys. Rev. X **10**, 031011 (2020).
[23] H. J. Kimble, Nature (London) **453**, 1023 (2008).
[24] P. Lodahl, S. Mahmoodian, S. Stobbe, A. Rauschenbeutel, P. Schneeweiss, J. Volz, H. Pichler, and P. Zoller, Nature (London) **541**, 473 (2017).
[25] D. Roy, C. M. Wilson, and O. Firstenberg, Rev. Mod. Phys. **89**, 021001 (2017).
[26] D. E. Chang, J. S. Douglas, A. González-Tudela, C.-L. Hung, and H. J. Kimble, Rev. Mod. Phys. **90**, 031002 (2018).
[27] S. Ritter, C. Nölleke, C. Hahn, A. Reiserer, A. Neuzner, M. Uphoff, M. Mücke, E. Figueroa, J. Bochmann, and G. Rempe, Nature (London) **484**, 195 (2012).
[28] P. Lodahl, Quantum Sci. Technol. **3**, 013001 (2018).
[29] Q. Y. Cai and W. Z. Jia, Phys. Rev. A **104**, 033710 (2021).
[30] X. Zhang, C. Liu, Z. Gong, and Z. Wang, Phys. Rev. A **108**, 013704 (2023).
[31] X. Li, W. Zhao, and Z. Wang, Opt. Lett. **48**, 3595 (2023).
[32] D. F. Walls and G. J. Milburn, *Quantum Optics*, 2nd ed. (Springer, Berlin, 2008).
[33] T. Petrosky and S. Subbiah, Phys. E (Amsterdam, Neth.) **19**, 230 (2003).
[34] A. Frisk Kockum, P. Delsing, and G. Johansson, Phys. Rev. A **90**, 013837 (2014).
[35] A. F. Kockum, G. Johansson, and F. Nori, Phys. Rev. Lett. **120**, 140404 (2018).
[36] P. Türschmann, H. L. Jeannic, S. F. Simonsen, H. R. Haakha, S. Götzinger, V. Sandoghdar, P. Lodahl, and N. Rotenberg, Nanophotonics **8**, 1641 (2019).
[37] G. Andersson, B. Suri, L. Z. Guo, T. Aref, and P. Delsing, Nat. Phys. **15**, 1123 (2019).
[38] A. González-Tudela, C. S. Muñoz, and J. I. Cirac, Phys. Rev. Lett. **122**, 203603 (2019).
[39] S. Guo, Y. Wang, T. Purdy, and J. Taylor, Phys. Rev. A **102**, 033706 (2020).
[40] B. Kannan, M. J. Ruckriegel, D. L. Campbell, A. F. Kockum, J. Braumüller, D. K. Kim, M. Kjaergaard, P. Krantz, A. Melville, B. M. Niedzielski, A. Vepsäläinen, R. Winik, J. L. Yoder, F. Nori, T. P. Orlando, S. Gustavsson, and W. D. Oliver, Nature (London) **583**, 775 (2020).
[41] R. Bag and D. Roy, Phys. Rev. A **108**, 053717 (2023).
[42] L. Z. Guo, A. F. Kockum, F. Marquardt, and G. Johansson, Phys. Rev. Res. **2**, 043014 (2020).
[43] S. Longhi, Opt. Lett. **46**, 2091 (2021).
[44] Q.-Y. Qiu, Y. Wu, and X.-Y. Lü, Sci. China: Phys., Mech. Astron. **66**, 224212 (2023).
[45] K. H. Lim, W.-K. Mok, and L.-C. Kwek, Phys. Rev. A **107**, 023716 (2023).
[46] A. Carollo, D. Cilluffo, and F. Ciccarello, Phys. Rev. Res. **2**, 043184 (2020).
[47] A. A. Abdumalikov, Jr., O. Astafiev, A. M. Zagoskin, Yu. A. Pashkin, Y. Nakamura, and J. S. Tsai, Phys. Rev. Lett. **104**, 193601 (2010).
[48] A. M. Vadiraj, A. Ask, T. G. McConkey, I. Nsanzineza, C. W. Sandbo Chang, A. F. Kockum, and C. M. Wilson, Phys. Rev. A **103**, 023710 (2021).
[49] W. Zhao, Y. Zhang, and Z. Wang, Front. Phys. **17**, 42506 (2022).
[50] X. Wang, T. Liu, A. F. Kockum, H.-R. Li, and F. Nori, Phys. Rev. Lett. **126**, 043602 (2021).
[51] X. Wang and H. R. Li, Quantum Sci. Technol. **7**, 035007 (2022).
[52] N. Liu, X. Wang, X. Wang, X. S. Ma, and M.-T. Cheng, Opt. Express **30**, 23428 (2022).
[53] X. Wang, Z.-M. Gao, J.-Q. Li, H.-B. Zhu, and H.-R. Li, Phys. Rev. A **106**, 043703 (2022).
[54] A. Soro and A. F. Kockum, Phys. Rev. A **105**, 023712 (2022).
[55] L. Du, M.-R. Cai, J.-H. Wu, Z. Wang, and Y. Li, Phys. Rev. A **103**, 053701 (2021).
[56] L. Du and Y. Li, Phys. Rev. A **104**, 023712 (2021).
[57] H. Yu, Z. Wang, and J.-H. Wu, Phys. Rev. A **104**, 013720 (2021).
[58] F. D. M. Haldane and S. Raghu, Phys. Rev. Lett. **100**, 013904 (2008).
[59] S. Raghu and F. D. M. Haldane, Phys. Rev. A **78**, 033834 (2008).
[60] K. Y. Bliokh, D. Smirnova, and F. Nori, Science **348**, 1448 (2015).
[61] K. Y. Bliokh, F. J. Rodríguez-Fortuño, F. Nori, and A. V. Zayats, Nat. Photon. **9**, 796 (2015).
[62] K. Y. Bliokh, D. Leykam, M. Lein, and F. Nori, Nat. Commun. **10**, 580 (2019).
[63] T. Ozawa, H. M. Price, A. Amo, N. Goldman, M. Hafezi, L. Lu, M. C. Rechtsman, D. Schuster, J. Simon, O. Zilberberg, and I. Carusotto, Rev. Mod. Phys. **91**, 015006 (2019).
[64] M. Jangjan and M. V. Hosseini, Sci. Rep. **10**, 14256 (2020).
[65] M. Jangjan and M. V. Hosseini, Sci. Rep. **11**, 12966 (2021).
[66] M. Jangjan and M. V. Hosseini, Phys. Rev. B **106**, 205111 (2022).
[67] M. Jangjan, L. E. F. Foa Torres, and M. V. Hosseini, Phys. Rev. B **106**, 224306 (2022).
[68] X. Gu, S. Chen, and Y.-X. Liu, arXiv:1711.06829.
[69] W. Cai, J. Han, F. Mei, Y. Xu, Y. Ma, X. Li, H. Wang, Y. P. Song, Z.-Y. Xue, Z.-Q. Yin, S. Jia, and L. Sun, Phys. Rev. Lett. **123**, 080501 (2019).
[70] W. P. Su, J. R. Schrieffer, and A. J. Heeger, Phys. Rev. Lett. **42**, 1698 (1979).
[71] H. S. Xu, K. L. Zhang, L. Jin, and Z. Song, Phys. Rev. A **105**, 033501 (2022).

[72] L. Jin, Phys. Rev. A **96**, 032103 (2017).
[73] L. Jin and Z. Song, Phys. Rev. B **99**, 081103(R) (2019).
[74] H. C. Wu, L. Jin, and Z. Song, Phys. Rev. B **103**, 235110 (2021).
[75] L. C. Wang, Y. Chen, M. Gong, F. Yu, Q. D. Chen, Z. N. Tian, X. F. Ren, and H. B. Sun, Phys. Rev. Lett. **129**, 173601 (2022).
[76] R. Fleury and A. Alú, Phys. Rev. B **87**, 045423 (2013).
[77] C. Valagiannopoulos, Phys. Rev. B **101**, 195301 (2020).
[78] E. Kim, X. Y. Zhang, V. S. Ferreira, J. Banker, J. K. Iverson, A. Sipahigil, M. Bello, A. González-Tudela, M. Mirhosseini, and O. Painter, Phys. Rev. X **11**, 011015 (2021).
[79] U. Fano, Phys. Rev. **124**, 1866 (1961).
[80] A. E. Miroshnichenko, S. F. Mingaleev, S. Flach, and Y. S. Kivshar, Phys. Rev. E **71**, 036626 (2005).
[81] M. V. Gustafsson, T. Aref, A. F. Kockum, M. K. Ekström, G. Johansson, and P. Delsing, Science **346**, 207 (2014).
[82] Z.-Q. Wang, Y.-P. Wang, J. Yao, R.-C. Shen, W.-J. Wu, J. Qian, J. Li, S.-Y. Zhu, and J. Q. You, Nat. Commun. **13**, 7580 (2022).
[83] P. Roushan, C. Neill, J. Tangpanitanon, V. M. Bastidas, A. Megrant, R. Barends, Y. Chen, Z. Chen, B. Chiaro, A. Dunsworth *et al.*, Science **358**, 1175 (2017).
[84] X. Zhang, E. Kim, D. K. Mark, S. Chol, and O. Painter, Science **379**, 278 (2023).